

Absolute left-handed behaviors in a triangular elliptical-rod photonic crystal

Zhixiang Tang, Runwu Peng and Dianyuan Fan

Shanghai Institute of Optics and Fine mechanics, Chinese Academy of Science, Shanghai 201800, China
tangzx1000@163.com

Shuangchun Wen

School of Computer and Communication, Hunan University, Changsha 410082, China

Hao Zhang and Liejia Qian

Department of Optical Science and Engineering, Fudan University, Shanghai 200433, China

Abstract: In this paper we theoretically study the left-handed behaviors in a two-dimensional triangular photonic crystal made of elliptical rods in air. An absolute left-handed region is found in the second photonic band by using the plane wave expansion method to analyze the photonic band structure and equifrequency contours. Typical left-handed behaviors such as negative refraction, flat superlensing and plano-concave lensing are demonstrated by the finite-difference time-domain simulations. These behaviors are also compared with the quasi-negative refraction and the resulted focusing effects in a square-lattice two-dimensional photonic crystal.

© 2005 Optical Society of America

OCIS CODES: (160.4760) Optical materials; (230.3990) Microstructure devices

References and links

1. V. G. Veselago, "The electrodynamics of substances with simultaneously negative values of ϵ and μ ," *Sov. Phys. Usp.* **10**, 509-514 (1968).
2. R. A. Shelby, D. R. Smith and S. Schultz, "Experimental verification of a negative index of refraction," *Science* **292**, 77-79 (2001).
3. Hongsheng Chen, Lixin Ran, Jiantao, Huangfu, Xianmin Zhang, Kangsheng Chen, Tomasz M. Grzegorzczak and Jin Au Kong, "Left-handed materials composed of only S-shaped resonators," *Phys. Rev. E* **70**, 057605 (2004).
4. Ertugrul Cubukcu, Koray Aydin, Ekmel Ozbay Stavroula Foteinopoulou and Costas M. Soukoulis, "Negative refraction by photonic crystals," *Nature* **423**, 604-605 (2003).
5. Patanjali V. Parimi, Wentao T. Lu, Plarenta Vodo and Srinivas Sridhar, "Imaging by flat lens using negative refraction," *Nature* **426**, 404 (2003).
6. N. Seddon and T. Bearpark, "Observation of the inverse Doppler effect," *Science* **302**, 1537-1540 (2003).
7. Evan J. Reed, Marin Soljacic and John D. Joannopoulos, "Reversed Doppler effect in photonic crystals," *Phys. Rev. Lett.* **91**, 133901 (2003).
8. Chiyan Luo, Mihai Ibanescu, G. Johnson and J. D. Joannopoulos, "Cerenkov radiation in photonic crystals," *Science* **299**, 368-371 (2003).
9. J. B. Pendry, "Negative refraction makes a perfect lens," *Phys. Rev. Lett.* **85**, 3966-3969 (2000).
10. P. Vodo, P. V. Parimi, W. T. Lu and S. Sridhar, "Focusing by planoconcave lens using negative refraction," *Appl. Phys. Lett.* **86**, 201108 (2005).
11. C. G. Parazzoli, R. B. Greigor, J. A. Nielsen, M. A. Thompson, K. Li, A. M. Vetter, M. H. Tanielian and D. C. Vier, "Performance of a negative index of refraction lens," *Appl. Phys. Lett.* **84**, 3232-3234 (2004).
12. Nicholas Fang, Hyesog Lee, Cheng Sun and Xiang Zhang, "Sub-diffraction-limited optical imaging with a sliver superlens," *Science* **308**, 534-537 (2005).
13. M. Notomi, "Theory of light propagation in strongly modulated Photonic Crystals: refractionlike behavior in the vicinity of the photonic band gap," *Phys. Rev. B* **62**, 10696-10705 (2000).
14. S. Foteinopoulou and C. M. Soukoulis, "Negative refraction and left-handed behavior in two-dimensional Photonic Crystals," *Phys. Rev. B* **67**, 235107 (2003).

15. Pavel A. Belov, Constantin R. Simovski and Pekka Ikonen, "Canalization of subwavelength images by electromagnetic crystals," *Phys. Rev. B* **71**, 193105 (2005).
16. Alejandro Martinez and Javier Marti, "Analysis of wave focusing inside a negative photonic-crystal slab," *Opt. Express* **13**, 2858-2868 (2005), <http://www.opticsexpress.org/abstract.cfm?URI=OPEX-13-8-2858>.
17. Chiyan Luo, Steven G. Johnson, J. D. Joannopoulos and J. B. Pendry, "All-negative refraction without negative effective index," *Phys. Rev. B* **65**, 201104 (2002).
18. Chao-Hsien Kuo and Zhen Ye, "Flat lens imaging does not need negative refraction," *cond-mat/0312288* (2004).
19. Chao-Hsien Kuo and Zhen Ye, "Optical transmission of photonic crystal structures formed by dielectric crystals: Evidence for non-negative refraction," *Phys. Rev. E* **70**, 056608 (2004).
20. Hung-Ta Chien, Hui-Ting Tang, Chao-Hsien Kuo, Chii-Chang Chen and Zhen Ye, "Direct diffraction without negative refraction," *Phys. Rev. B* **70**, 113101 (2004).
21. Liang-Shan Chen, Chao-Hsien Kuo and Zhen Ye, "Guiding optical flows by Photonic Crystal slabs made of dielectric cylinders," *Phys. Rev. E* **69**, 066612 (2004).
22. Chao-Hsien Kuo and Zhen Ye, "Negative-refraction-like behavior revealed by arrays of dielectric cylinders," *Phys. Rev. E* **70**, 026608 (2004).
23. R. Moussa, S. Foteinopoulou, Lei Zhang, G. Tuttle, K. Guven, E. Ozbay and C. M. Soukoulis, "Negative refraction and superlens behavior in a two-dimensional Photonic Crystal," *Phys. Rev. B* **71**, 085106 (2005).
24. Shuai Feng, Zhi-Yuan Li, Zhi-Fang Feng, Bing-Ying Cheng and Dao-Zhong Zhang, "Imaging properties of an elliptical-rod photonic-crystal slab lens," *Phys. Rev. B* **72**, 075101 (2005).
25. A. Taflov, *Computational Electrodynamics: The Finite-Difference Time-Domain Method* (Artech House INC, Norwood, 1995).
26. J. P. Berenger, "A perfectly matched layer for the absorption of electromagnetic waves," *J. Comput. Phys.* **114**, 185-200 (1991).
27. K. Sakoda, *Optical Properties of Photonic Crystals* (Springer-Verlag, Berlin, 2001).
28. Zhaolin Lu, Caihua Chen, Christopher A. Schuetz, Shouyuan Shi, Janusz A. Murakowski, Garrett J. Schneider and Dennis W. Prather "Subwavelength imaging by a flat cylindrical lens using optimized negative refraction," *Appl. Phys. Lett.* **87**, 091907 (2005).
29. Xianyu Ao and Sailing He, "Negative refraction of left-handed behavior in porous alumina with infiltrated silver at an optical wavelength," *Appl. Phys. Lett.* **87**, 101112 (2005).
30. Sanshui Xiao, Min Qiu, Zhichao Ruan and Sailing He, "Influence of the surface termination to the point imaging by a photonic crystals slab with negative refraction," *Appl. Phys. Lett.* **85**, 4269-4271 (2004).
31. X. Wang, Z. F. Ren and K.Kempa, "Unrestricted superlensing in a triangular two-dimensional photonic crystal," *Opt. Express* **12**, 2919-2924 (2004), <http://www.opticsexpress.org/abstract.cfm?URI=OPEX-12-13-2919>.
32. E. Cubukcu, K. Aydin, E. Ozbay, S. Foteinopoulou and C. M. Soukoulis, "Subwavelength Resolution in a Two-Dimensional Photonic-Crystal- Based Superlens," *Phys. Rev. Lett.* **91**, 207401 (2003).
33. Zhixiang Tang, Hao Zhang, Runwu Peng, Yunxia Ye, Lei Shen, Shuangchun Wen and Dianyuan Fan, "Two degenerate anisotropic modes in the experimental photonic crystal slab lens," submitted to *Opt. Commun* (2005).

1. Introduction

Left-handed materials (LHMs) or negative refractive-index materials (NIMs), characterized by simultaneously negative permittivity and permeability, were initially proposed and theoretically analyzed by Veselago in the 1960s [1], and have recently attracted renewed interest because of the experimental progresses [2-5]. Unusual electromagnetic phenomena, such as negative refraction, reversed Doppler shift [6,7] and reversed Cerenkov radiation [8], could be expected in LHMs, which can be applied to fabricate the flat superlens [9] and plano-concave lens [10,11]. Perhaps the most exciting application of LHMs is the possibility of perfect lens that overcomes the diffraction limit by regenerating the entire spectrum of the source at the image plane [9, 12]. Due to the absence of LHMs in nature, various approaches have been proposed to fabricate the equivalent metamaterial. In one approach, a metamaterial with negative refraction, made of a periodic array of split ring resonators (SRRs) and thin wires, was first demonstrated experimentally at microwave frequency [2]. Recently, a new simple structure only with S-shaped resonators has been designed, and negative refraction was demonstrated experimentally [3].

Due to its dispersion characteristics, photonic crystal (PhC) is an alternative for the realization of LHMs. Notomi's theoretical works indicated that left-handed behaviors in PhCs

are possible in the regimes of negative group velocity and negative effective index above the first band near the Brillouin-zone center Γ [13]. Soon after the experimental observation of negative refraction in PhCs [4], Parimi *et al.* demonstrated the imaging phenomenon by flat PhC lenses [5].

In general, there are two kinds of negative refraction (and its resulted focusing effects) in PhC structures [14-17]. One is left-handed behavior as being described by Veselago [1]. In this case, the electromagnetic fields \mathbf{E} , \mathbf{H} and the wave vector \mathbf{k} form a left-handed triplet (i.e., $\mathbf{S} \cdot \mathbf{k} < 0$, where \mathbf{S} is the Poynting vector). The other negative refraction is realized without employing negative index or a left-handed behavior, but by the high order Bragg scattering [14] or anisotropy [17]. In the latter case, the PhC behaves much like a right-handed medium (i.e., $\mathbf{S} \cdot \mathbf{k} > 0$). This kind of quasi-negative refraction and its resulted focusing effects, caused by anisotropy in square-lattice PhCs, have been investigated systematically by Kuo *et al.* [18-22].

Recently, Moussa *et al.* theoretically and experimentally demonstrated left-handed behaviors such as negative refraction and superlensing in a triangular lattice of rectangular dielectric rods [23]. Subsequently, reference [24] analyzed imaging properties of a square-lattice elliptical-rod PhC slab lens that was based on the quasi-negative refraction caused by anisotropy [15, 17]. Although we knew that the noncircular rods would result in a left-handed frequency region, it is still quite interesting to optimize the left-handed behaviors. For this purpose, in this paper we theoretically investigate a left-handed two-dimensional (2D) PhC that is made of the elliptical rods arranged in a triangular lattice in air. Typical left-handed behaviors such as negative refraction, flat superlensing and plano-concave lensing are demonstrated by numerical simulations using the finite-difference time-domain method (FDTD) [25]. We also compare these left-handed behaviors with the quasi-negative refraction and its resulted focusing effects.

The rest of this paper is organized as follows. In Section 2, we theoretically analyze this PhC by examining the photonic band structure and equipfrequency contours (EFCs). The FDTD simulation results of negative refraction, flat lensing and plano-concave lensing are shown in Section 3. A comparison between left-handed behaviors and quasi-negative refractions is also made. Finally, the conclusions are given in Sec. IV.

2. Photonic band structure analysis

The 2D PhC considered in this paper consists of a triangular lattice of elliptical rods arranged in the background of air. The dielectric constant of these rods is $\epsilon = 12.96$. The dimensions of each rod in x and y directions are set: major axis $r_x = a$ and minor axis $r_y = 0.5a$, where a is the lattice constant. This structure is schematically shown in Fig. 1(a). For this elliptical-rod structure, we only consider the TM polarization that the electric field E_z is parallel to these rods.

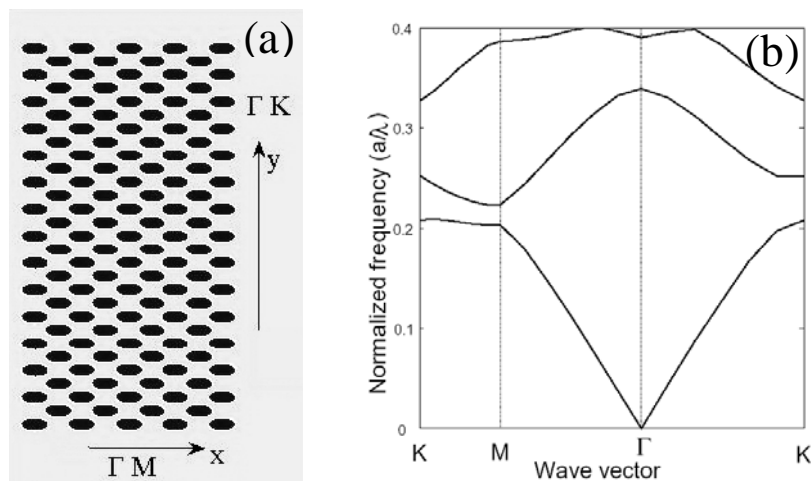


Fig. 1. (a) Schematics of a triangular of array elliptical rods in air. (b) The photonic band structure for the TM polarization.

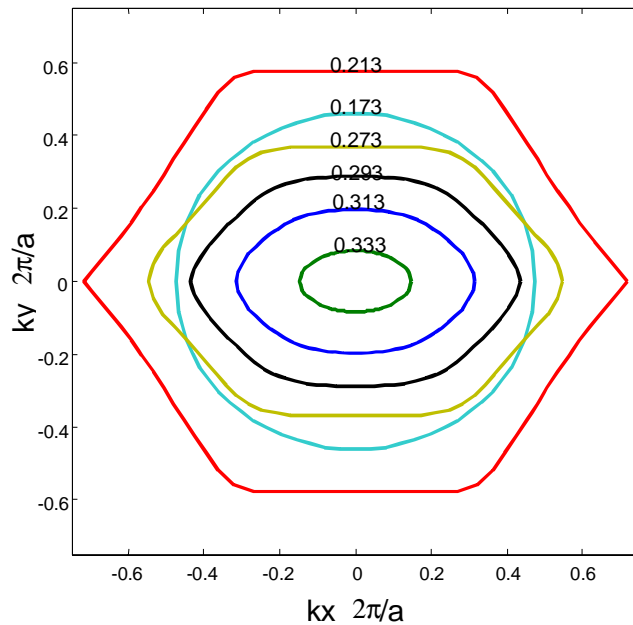


Fig. 2. Several EFCs of the lowest two bands for the TM polarization.

The photonic band structure and EFCs are calculated by the plane wave expansion method and plotted in Fig. 1(b) and Fig. 2, respectively. 961 plane waves are employed to assure the convergence of numerical calculations. The frequencies are normalized as a/λ . Figure 2 clearly shows that EFC of a region in the second band shrinks with increasing frequency, which indicates that the PhC is left-handed. Similar to the case of rectangular rods, but different from the case of circular rods, EFCs of our PhC are not totally isotropic because of the break in symmetry [23]. The effective index n_{eff} in this frequency region, extending from 0.26 to 0.33, is shown in Fig. 3. The normalized frequency $\omega_0 = 0.313$, where the effective index is $n_{eff} = -1$, is the optimal frequency for superlensing. Based on EFC at this frequency, the angle-dependent effective index $n_{eff}(\omega_0, \theta)$ is calculated and plotted in Fig. 4. Because of anisotropy, $n_{eff}(\omega_0, \theta)$ varies between -0.63 and -1.05 with the angle θ formed by the wave vector $\mathbf{k}(\omega_0)$ and ΓM .

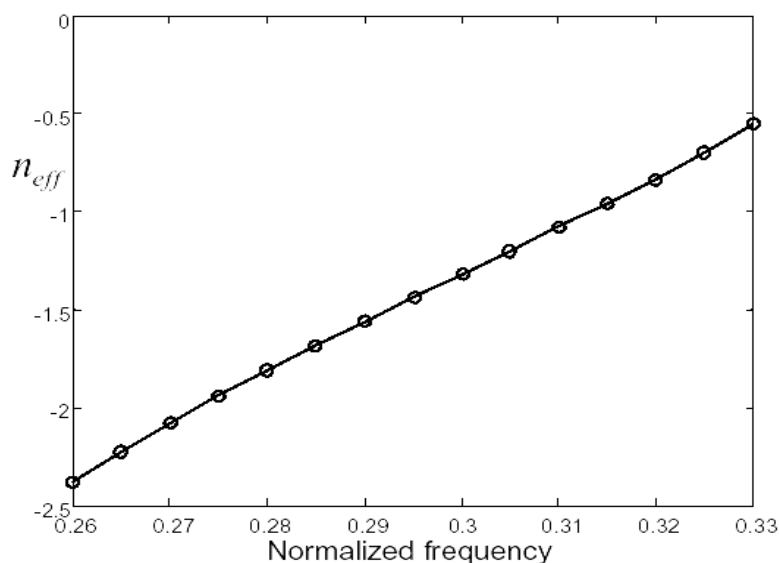


Fig. 3. Effective index of the second band vs. the normalized frequency.

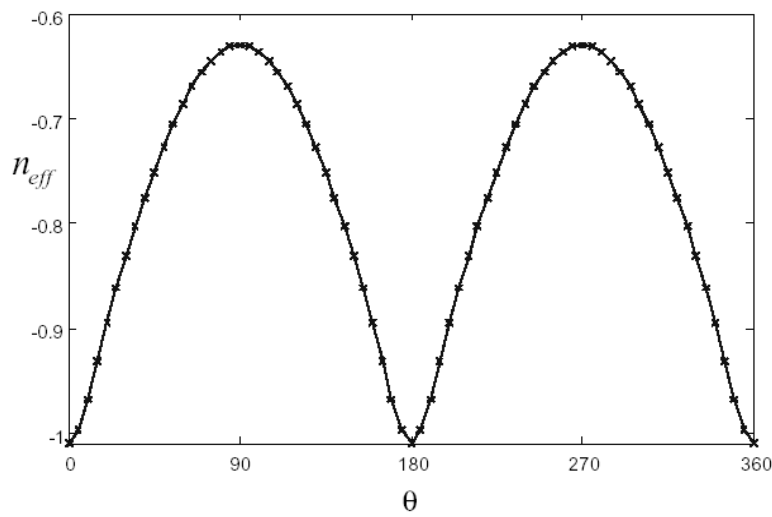


Fig. 4. The calculated effective index $n_{eff}(\theta)$ at the optimal frequency $\omega_0=0.313$.

3. Numerical simulations

To study the left-handed behaviors in this PhC, numerical simulations are conducted using the FDTD method. In all numerical simulations, the boundaries are perfectly matched layers (PMLs) [26]. Considering the symmetry of Bloch modes of this PhC, the interface between PhC and free space is arranged along ΓK [27].

3.1 Negative refraction

Numerical simulations of negative refraction are illustrated in Fig. 5. A Gaussian beam with a normalized frequency $\omega_0=0.313$ is incident to the PhC with angles $\varphi = 30^\circ$ and $\varphi = 60^\circ$ to the normal of the interface, as shown in Fig. 5(a) and Fig. 5(b), respectively. In both of the two circumstances, the incident beams are refracted in the opposite directions of the reflected beams, namely, the effective index of this PhC slab is $n_{eff} = -1$. This kind of negative refraction is a pure left-handed behavior that corresponds to $\mathbf{v}_g \cdot \mathbf{k} < 0$, which is different from the quasi-negative refraction caused by anisotropy in the first partial band gap of a square-lattice PhC. In the square-lattice PhCs, the first partial band gap results in an anisotropic response and canalization effect. Because transmitted waves in this PhC are all confined in the canalized direction, incident beams are compelled to refract in this direction independent of the incident angles [20]. Since all refracted beams transmit at the prearranged direction controlled by the PhC orientation, this quasi-negative refraction is governed by the canalization effect and does not obey the Snell's law.

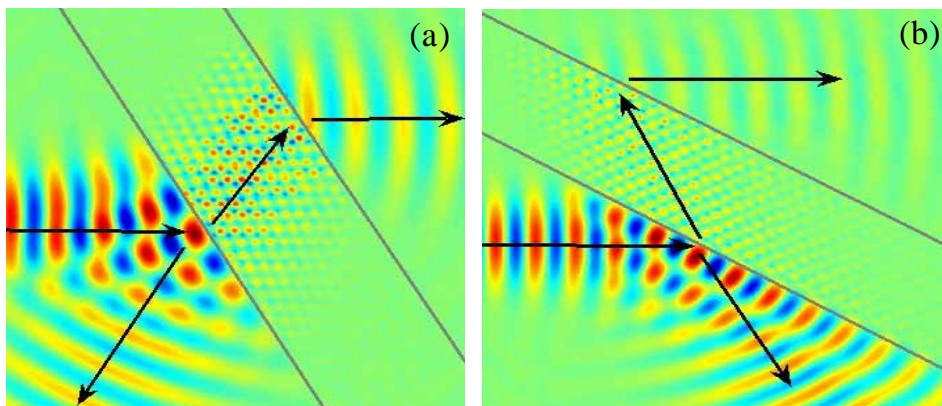


Fig. 5. Negative refractions for two incident angles: (a) $\varphi = 30^\circ$ and (b) $\varphi = 60^\circ$.

Superlensing is the most attractive application of LHMs [28, 29]. Figure 6 shows the flat superlens made by this PhC based on the absolutely left-handed behavior. Figure 6(a1) and (b1) give the snapshots of the electric fields, while Fig. 6(a2) and (b2) give the corresponding normalized average intensities over a period. Figure 6(a2) and (b2) are combinations of three parts including the normalized intensity of the source field, the field in the flat lens and the image field. The PhC structure, which is sketched by wine-colored ellipses, is cut $0.25a$ at each interface for exciting the surface waves [23, 30]. A continuous-wave point source is located at the left side of the PhC slab with the normalized frequency $\omega_0 = 0.313$. In Fig. 6(a) and (b), the distances from the point source to the first interface of the PhC slab (i.e. the object distance) are $d_o = 2.75a$ and $d_o' = 4.75a$, and the images are formed at $d_i = 2.30a$ and $d_i' = 0.45a$ away from the second interface, respectively. It is obvious that the distances satisfy a relationship $d_o + d_i \cong d_o' + d_i'$, which is required by the Snell's law for a flat lens with $n_{eff} = -1$. Particularly, there is an internal focus inside the PhC slab, which is a clear evidence of LHMs following the rules of geometric optics. The transverse normalized field intensities of the source and the images are shown in Fig. 7. Similar to Ref. [23, 30], the full width at the half maximum (FWHM) of the image decreases from 0.50λ to 0.39λ when the PhC is cut $0.25a$ at each interface.

However, there is another different flat superlens that does belong to the left-handed behavior. Based on the canalization effect caused by the first partial band gap of a square-lattice PhC, several flat superlenses have been demonstrated theoretically and experimentally [31, 32]. For this kind of superlens, most of the spatial spectrum of the source is coupled into the canalization at the incident interface, tunneled through the PhC slab, and finally ejected out from the other interface [15]. The image is formed near the interface and independent of the object distance. Because the evanescent waves are not amplified, this superlens overcomes the diffraction limit only in the near field region and the source must be located near the flat lens for effectively coupling with evanescent waves.

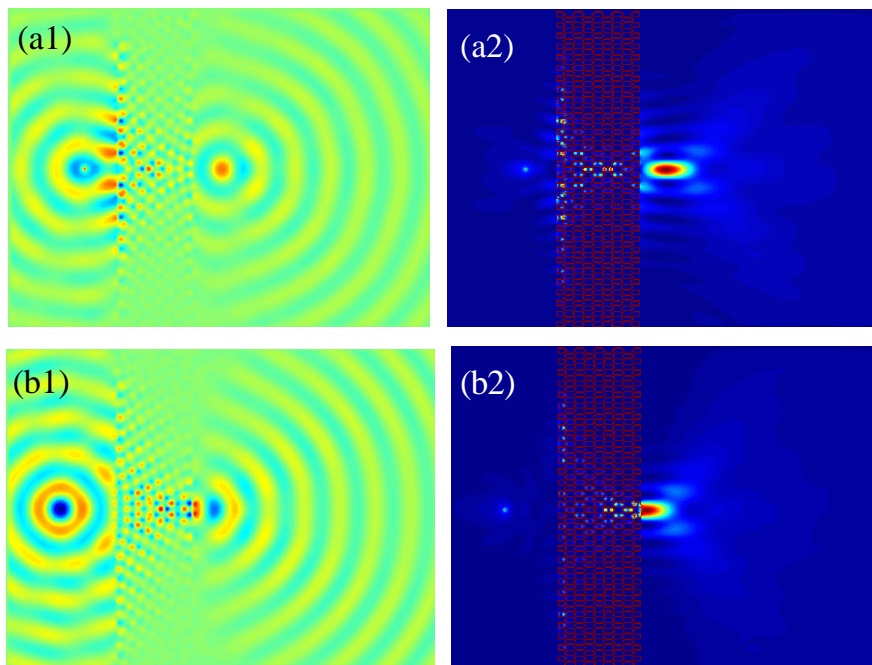


Fig. 6. The propagation maps for the flat superlens. The object distance is $d_o = 2.75a$ for (a) and $d_o' = 4.75a$ for (b). (a1) and (b1) are the snapshots of the electric field. (a2) and (b2) display the corresponding normalized average intensities over a period.

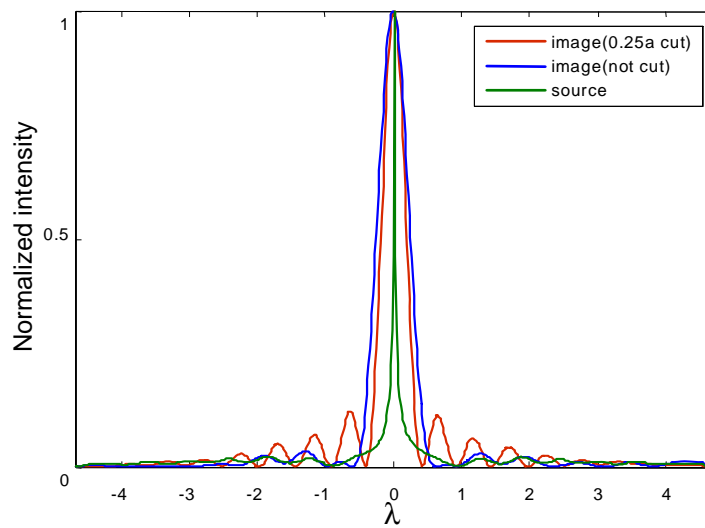


Fig. 7. The transverse normalized field intensities of the source and the images.

3.3 Plano-concave lens

Plano-concave lens is another typical application of LHMs. LHMs allows focusing of a plane wave by concave rather than convex surface. Vodo [10] and Parazzoli [11] have fabricated plano-concave lenses by using SRRs and photonic crystals, respectively. It should be mentioned that there is a right-handed mode coexisted in the left-handed frequency region for square-lattice PhCs such as Vodo's plano-concave lens and Parimi's flat lens. (More details will be shown in our another study [33].) Because of not being a really all-angle negative refraction, the quasi-negative refraction PhC cannot be used to fabricate plano-concave lens.

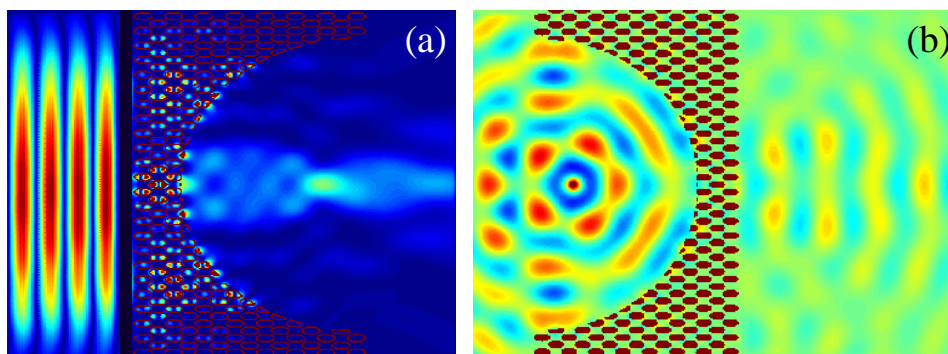


Fig. 8. (a) Focusing by plano-concave lens. (b) Field maps of the incident point source and the emerging plane wave.

Plano-concave lenses made by this PhC are shown in Fig. 8. The PhC plano-concave lenses are sketched by wine-colored ellipses too. In Fig. 8(a), a Gaussian beam with normalized frequency $\omega_0 = 0.313$ incidents into the PhC plano-concave lens perpendicularly, and a focus is formed. Similar to Ref. [10], this photograph is composed of two surface plots. On the left hand of the dark strip, the field map of incident beam is shown, and on the right side is the average intensity over a period. In Fig. 8(b), a continuous-wave point source is located on the focus, and the plane wave is formed out of the plano-concave lens. Because of anisotropy, the focus is not exactly located at $R / |1-n|$ (i.e., $R / 2$).

4. Conclusions

In this paper we have systematically investigated typical left-handed behaviors in a 2D PhC that is made of elliptical rods arranged in a triangular lattice in air. An effective index $n_{eff} = -1$

has been found in the second photonic band by analyzing the photonic band structure and EFCs, which are calculated by the plane wave expansion method. Typical left-handed behaviors such as negative refraction, flat superlensing and plano-concave lensing have been demonstrated by the FDTD simulations. We also have compared these behaviors with the quasi-negative refraction and its resulted focusing effects in a square-lattice 2D PhC, which are caused by anisotropy in the first partial band gap.

Acknowledgments

This work is partially supported by the Natural Science Foundation of China (Grant Nos. 10576012 and 60538010), the National High Technology Research and Development Program of China (Grant No. 2004AA84ts12), and the Specialized Research Fund for the Doctoral Program of Higher Education of China (Grant No. 20040532005). We acknowledge Dr. Shangping Guo for valuable suggestions and discussions.